Comparative seismic performance of a moment frame equipped with Lateral Impact Resilient Double Concave Frictional devices

Available online at www.sciencedirect.com

ScienceDirect

Procedia Structural Integrity 44 (2023) 1466–1473

Structural Integrity Procedia

www.elsevier.com/locate/procedia

XIX ANIDIS Conference, Seismic Engineering in Italy

Comparative seismic performance of a moment frame equipped with Lateral Impact Resilient Double Concave Frictional devices

Gaspar Auad[a, b,*], Paolo Castaldo[a], José L. Almazán[b]

[a]*Politecnico di Torino, Corso Duca degli Abruzzi 24, Turin (10129), Italy*
[b]*Pontificia Universidad Católica de Chile, Vicuña Mackenna 4860, Santiago (8970117)*

Abstract

This study presents a comparative assessment of the seismic performance of a reinforced concrete moment frame equipped with a new isolator. The Lateral Impact Resilient Double Concave Friction Pendulum (LIR-DCFP) bearing has an enhanced inner slider capable of limiting the magnitude of the lateral impact force generated between the inner slider and the restraining rims of the sliding surfaces. Due to the presence of a plane high-friction interface with an internal gap, the novel isolator has an increased energy dissipation capacity that is activated during the lateral impact. Three isolation systems were considered to evaluate the benefits of using LIR-DCFP devices. One conformed by the suggested isolator, and two composed of classic non-articulated Double Concave Friction Pendulum (DCFP) bearings. The isolation devices were modelled employing a numerical formulation based on rigid body dynamics, capable of accounting for the lateral impact behaviour. The superstructure, a reinforced concrete moment resisting frame designed according to the American ASCE/SEI 7-16 standard, was modelled using beam-column elements considering geometric and material nonlinearities. Furthermore, the degrading behaviour of the building was incorporated using a proper degradation model for both the stiffness and the force. Incremental Dynamic Analyses (IDAs) were performed considering the friction coefficient as a random variable to characterize the statistics of the maximum inter-story responses. With the data generated in the IDAs, fragility curves related to the superstructure performance were constructed. Finally, employing the hazard curve, reliability curves were derived. The superstructure equipped with LIR-DCFP bearings presents better seismic performance than the same building equipped with the same size DCFP isolators. The benefits of using the new isolator are not achieved by increasing the lateral capacity of the classic isolation system.

Peer-review under responsibility of the scientific committee of the XIX ANIDIS Conference, Seismic Engineering in Italy.

Keywords: LIR-DCFP isolator; internal lateral impact; high-friction interface; internal gap; seismic reliability; inter-story drift demand.

* Corresponding author. Tel.: +56 9 30831472
E-mail address: gaspar.auadalvarez@polito.it / gaauad@uc.cl

Peer-review under responsibility of the scientific committee of the XIX ANIDIS Conference, Seismic Engineering in Italy.
10.1016/j.prostr.2023.01.188

1. Introduction

One of the most valuable ways of protecting non-slender structures subjected to high magnitude ground motions is seismic isolation. One device usually employed in constructing the isolation level is the Friction Pendulum System (FPS), suggested by Zayas et al. (1990). This device consists of an articulated slider and a spherical surface that provide re-centering forces and energy dissipation through the relative sliding between these two bodies. Unlike the FPS bearings, having only one sliding surface, other frictional isolators have been proposed based on multiple sliding surfaces. Two of the most used devices in this last category are the Double Concave Friction Pendulum (DCFP), analyzed by Fenz and Constantinou (2006), and the Triple Friction Pendulum (TFP) bearing, studied by Fenz and Constantinou (2008). These isolators with multiple sliding surfaces exhibit passive adaptive behavior, a feature valuable to performing multi-objective designs.

Under extreme ground motions, isolation systems formed by frictional isolators may develop excessive base displacement (Hall et al. (1995); Mazza and Vulcano (2012); Mazza (2018)). If the lateral capacity of the isolation system is overcome, the internal lateral impact between the inner sliders and the restraining rims of sliding surfaces can be observed. Bao et al. (2017) and Becker et al. (2017) studied that those internal impacts are one of the most important causes of the failure of DCFP and TFP bearings. Typically, these impacts generated inside the isolation system can jeopardize the benefits of using seismic isolation by increasing the ductility demand on the superstructure.

Recently, a new device proposed by Auad and Almazán (2021) was suggested as an alternative to mitigate the adverse effects of internal lateral impacts. The Lateral Impact Resilient Double Concave Friction Pendulum (LIR-DCFP) bearing has an enhanced inner slider capable of limiting the magnitude of the impact forces and dissipating an additional amount of energy. The inner slider consists of two rigid bodies (the top and bottom sliders) that are in contact generating a plane high-friction interface. To ensure an effective design of the device, the high friction sliding between the top and bottom slider must occur only under the presence of an internal impact. Auad and Almazán (2021) only studied one structure subjected to three seismic records was analyzed. More deterministic and probabilistic analyses must be performed to assess the benefits of using the novel frictional isolator.

A reliability-based comparison of the seismic performance in terms of maximum inter-story drift demand of a reinforced concrete moment-resisting frame equipped with frictional isolators is presented in this paper. Three isolation systems were considered, one formed by LIR-DCFP bearings and two formed by DCPF bearings (one of them with a larger lateral capacity). The superstructure was designed according to the American Standard ASCE/SEI 7-16. An approach based on rigid body dynamics was employed to model the isolators. The approach incorporates important modeling aspects such as uplifting, sticking-sliding phases, large displacement effects, and $P-\Delta$ effects. Two-dimensional Euler-Bernoulli beam-columns elements (Bao and Becker (2018)), capable of accounting for geometric and material nonlinearities, were used to model the superstructure. The most relevant uncertainties, the value of the friction coefficient and the record-to-record variability, were included in the reliability analyses. The statistics of the maximum inter-story drift responses were estimated by performing Incremental Dynamic Analyses (IDAs). With the data generated with the IDAs, the construction of fragility curves related to different maximum inter-story drift thresholds was performed. Finally, the reliability curves of the three studied cases were derived using the hazard and fragility curves. The comparative assessment of the seismic performance of the three isolation systems was conducted using the described reliability curves.

2. The Later Impact Resilient Double Concave Friction Pendulum (LIR-DCFP) bearing

The new frictional isolator, the LIR-DCFP bearing, is composed of two identical concave plates with spherical sliding surfaces described by a radius of R. The critical feature of this device is its enhanced inner slider. Two rigid bodies form the slider: the top and bottom sliders. These two pieces are in contact, generating a plane high-friction interface with an internal gap that allows the relative displacement between them. The interactions between curved surfaces (i.e., between the concave plates and the spherical surfaces of the sliders) generate low friction forces characterized by the friction coefficient μ_d. The friction coefficient developed in the high-friction interface is

denoted by the symbol μ_s. If $\mu_s > \mu_d$, the relative displacement between the top and bottom slider will start only if the inner slider impacts the restraining rims of the sliding surfaces.

The lateral behavior of frictional isolators can be described by the pendular force f_p, the frictional force f_μ, and the rigid impact force f_i that the bearing transmits to the superstructure. The sum of these three forces leads to the total force transmitted by the bearing. The rigid impact force f_i is generated when the relative displacement between the top and bottom sliders overcomes the size of the internal gap. In Fig. 1, the normalized force-displacement relationship of the LIR-DCFP bearing is presented. While the vertical load applied on the top concave plate W normalizes the lateral force, the effective radius of the device R_{eff} normalizes the total lateral displacement (i.e., the displacement of the top plate relative to the ground). In Fig. 1, five points of the lateral behavior of the proposed device linked to different configurations of the frictional isolator are illustrated to interpret the force-displacement constitutive. Point (1) describes the beginning of the low friction sliding between the spherical surfaces. Point (2) depicts the impact between the inner slider and the restraining rims of the concave plates. Between points (1) and (2), the normalized frictional force equals the low friction coefficient, and the pendular force increases with a unitary normalized stiffness. Point (3) indicates the first lateral contact between the top slider and the restraining rims of the bottom slider. Note that the high-friction sliding (i.e., the path between points (2) and (3)) is characterized by the high-friction coefficient μ_s and a constant pendular force. The pendular force does not change because the vectors that describe the direction of contact between the different bodies of the isolator remain constant. The configuration illustrated in point (4) triggers a dramatic increment in the rigid impact force, increasing the total force generated in the LIR-DCFP isolator. Finally, point (5) describes the returning of the bottom slider to its original position. This path is described by a unitary pendular stiffness and a low friction coefficient.

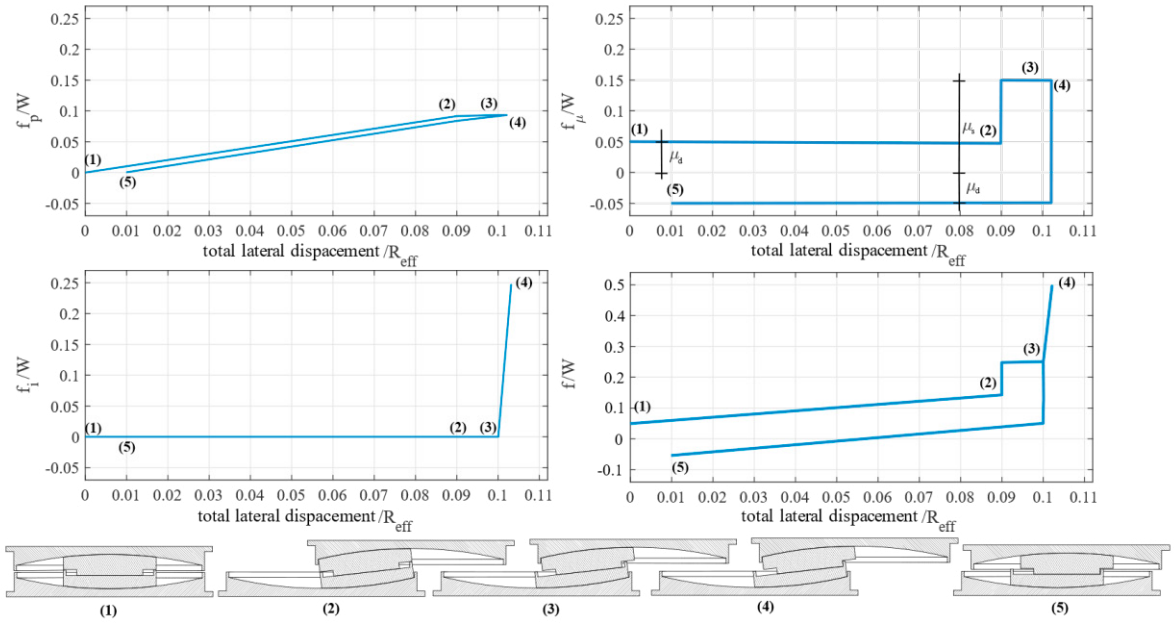

Fig. 1. Normalized force-displacement relationship of the LIR-DCFP isolator (modified from Auad and Almazan (2021))

3. Isolation systems considered and design of the reinforced concrete moment frame

The main objective of this study is to assess the benefits of using LIR-DCFP bearing instead of classical Double Concave Friction Pendulum (DCFP) isolators (Fenz and Constantinou (2006)). For this reason, three isolation systems are considered. The first two isolation systems correspond to isolation levels formed by the same size frictional devices. While LIR-DCFP bearings with internal gaps of 5 cm form the first isolation system, the second isolation system is formed by DCFP bearings. Considering these two isolation systems, no matter if LIR-DCPF or DCFP are employed, the first internal lateral impact between the inner slider and the restraining rims of the concave

plates will be observed at the same total lateral displacement of the device. Since the LIR-DCFP isolators with internal gaps form an isolation system with larger lateral capacity (i.e., this isolation level needs a larger base displacement to develop the rigid impact behavior), a third isolation system formed by DCFP bearing with larger concave plates is studied. The three considered isolators are shown in Fig. 2.

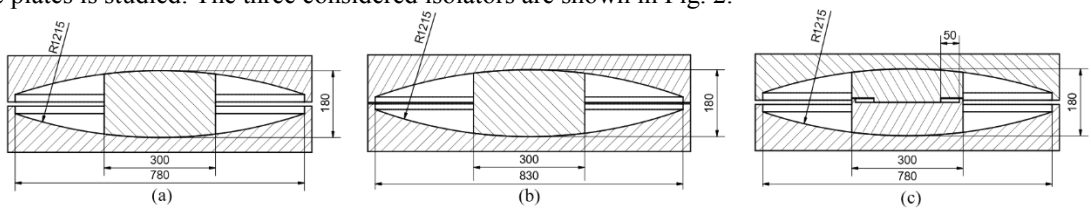

Fig. 2. Isolators used to form different isolation systems: (a) Same size DCFP bearing; (b) Larger size DCFP bearing; (3) LIR-DCPF with an internal gap of 5 cm. (All dimensions are in mm)

An approach based on rigid body dynamics (Auad & Almazán (2021); Bao & Becker (2019)) was employed to represent the isolation devices. This approach considers important modeling aspects such as the lateral impact behavior, large deformation, uplifting, partial uplifting, and P-Δ effects, among other essential phenomena. The beams and columns of the superstructure are modeled using two-dimensional Euler-Bernoulli beam-column elements in the state-space form (Bao & Becker, 2018). By using this beam-column formulation, it is possible to consider geometric effects since the co-rotational approach is used. Furthermore, the material nonlinearities are incorporated using the Bouc-Wen model with degrading behavior for both the force and stiffness.

The criteria of the AISC-SEI 7-16 standard were used to design the superstructure equipped with frictional isolators. Assuming that the building is located in Riverside (California) and is founded in stiff soil ($V_s = 530$ m/s), the equivalent lateral force procedure was used. The estimated maximum base displacement under the Maximum Considered Earthquake (MCE) was $D_M = 0.48$ m. This value was obtained using an effective radius of the isolators of $R_{eff} = 2.25$ m (isolated period of $T_b = 3$ sec) and a friction coefficient of $\mu_d = 0.04$ (the lower bound of the friction coefficient). The AISC-SEI 7-16 standard requires an increase of the base displacement to account for accidental torsion. Since two-dimensional structures are considered in this study, this increment is not considered. The base shear of the isolation system was estimated to be equal to 0.293 times the self-weigh of the structure using the maximum base displacement. This value was computed assuming a friction coefficient of $\mu_d = 0.08$ (the upper bound of the friction coefficient).

A reinforced concrete moment frame with three stories and two bays was designed using the estimated shear base under the action of the MCE. The bay and the story heigh of the superstructure are 8 m and 3.5 m, respectively. The self-weigh of the superstructure was taken equal to $W_s = 2{,}560$ kN. An illustration of the isolated building is presented in Fig. 3. Additionally, in Fig. 3, the reinforcement of the structural elements is shown

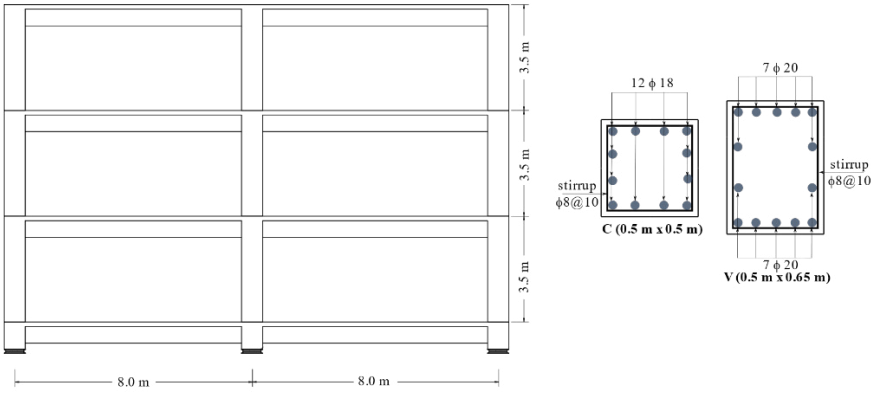

Fig. 3. Two-dimensional reinforced concrete moment frame equipped with frictional isolators

4. Uncertainties in the seismic reliability structures equipped with friction seismic isolators

Two of the most critical uncertainties in the seismic performance assessment of structures equipped with frictional isolators are the value of the friction coefficient and the record-to-record variability.

The sliding developed in frictional isolators is commonly modeled as a velocity-dependent model. In this study, the expression proposed by Mokha et al. (1990) and Constantinou et al. (1990) is employed to represent this dependency of the friction coefficient:

$$\mu_d = \mu_{max} - (\mu_{max} - \mu_{min})exp(-\alpha|\dot{v}|) \quad (1)$$

in which μ_{min} and μ_{max} are the sliding friction coefficient at slow and fast velocity $\dot{v}$, and α is the rate parameter. A random variable was used to represent the probabilistic distribution of μ_{max}. This random variable is characterized by an appropriate Gaussian PDF, truncated on both sides to 4% and 8% and with a mean value of 6%. Note that these two truncated sides are the lower and upper bounds of the friction coeffect used to design the isolation level lateral capacity and the elements of the superstructure. Eight values of μ_{max} were sampled using the Latin Hypercube Sampling (LHS) method. The probabilistic analyses were performed considering that the value of μ_{min} is correlated with the value of μ_{max} through a factor of 1/2 (i.e., $\mu_{min} = 1/2\mu_{max}$). In cases where the high-friction interface is considered, it is assumed that the high-friction coefficient is correlated with the sampled values of μ_{max} through a factor of 5/2 (i.e., $\mu_s = 5/2\mu_{max}$). The sliding between the top and bottom sliders of LIR-DCFP bearings is assumed not to be dependent on the velocity of sliding.

The record-to-record variability was considered by employing 23 seismic records. These records were modified to match the MCE spectrum related to the Riverside (California) site. The probabilistic analysis was performed, including an Intensity Measure (IM), aiming to separate the uncertainties of the input intensity and the characteristics of the records. In this study, the spectral acceleration at the isolated period $S_a(T_b)$ was chosen as the IM. Twelve values of the IM were used to conduct the analyses, ranging from $S_a(T_b) = 0.0.15$g to $S_a(T_b) = 0.47$g.

5. Incremental dynamic analyses (IDAs)

The first step to determining the statistics of the Engineering Demand Parameters (EDPs) of interest in terms of increasing IM levels is to conduct Incremental Dynamic Analyses (IDAs). In this study, three EDPs are studied: the maximum first inter-story drift $\delta_{max}^{(1)}$, the maximum second inter-story drift $\delta_{max}^{(2)}$, and the maximum third inter-story drift $\delta_{max}^{(3)}$. The statistics of the EDPs are assumed to follow lognormal distributions. Every EDP is fitted by calculating the sample lognormal mean $mean_{ln}(EDP)$ and the sample lognormal standard deviation $\sigma_{ln}(EDP)$. These two parameters are fitted employing the maximum likelihood estimation method. The samples are those obtained without considering the collapse cases. The collapse is monitored if one inter-story response exceeds 3% or if the explicit failure of one frictional isolator is detected (Bao & Becker (2019)). The samples of the EDPs are obtained by repeatedly solving the equation of motion. One IDA consists of 2,208 numerical simulations, combining the 23 seismic records scaled to the 12 levels of the IM with the eight sampled values of μ_{max}.

The Incremental Dynamics Analysis curves in terms of the maximum inter-story drifts responses of the three considered base-isolated structures are shown in Fig. 4. In general, the plastic displacement of the superstructure is concentrated in the first story (Fig. 4(a)) and decreases as the height of the structure rises. The EDPs response increases for higher values of the IM. Note that reductions of the 84th percentile of the second and third maximum inter-story drifts for large values of $S_a(T_b)$ are shown in Fig. 4((b) and (c)). These reductions are a consequence of the increasing collapse cases monitored. Significant reductions in the maximum inter-story responses are obtained by using LIR-DCFP bearings. The curves related to the isolation system formed by the suggested isolators are below those curves related to classical DCFP isolator for IM values higher than $S_a(T_b) = 0.26$g. At this level of the IM, the first internal impacts between the inner sliders and the restraining rims are detected, showing that using LIR-DCFP isolators is an effective alternative to mitigate the adverse effects of internal impacts. Increasing the size of the concave plates leads to a reduction of the statistical parameters of the EDPs. However, the reduction of the

maximum inter-story drift response achieved by using larger isolators is lower than that obtained by incorporating the high-frictional interface inside the isolation devices.

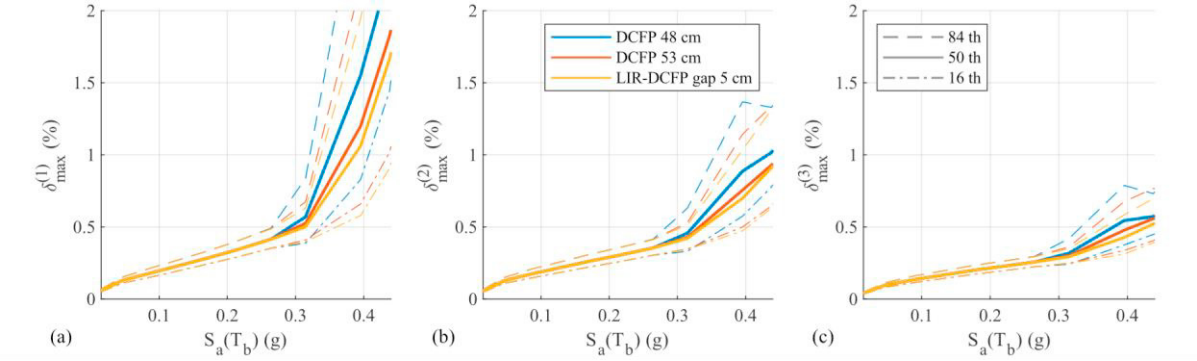

Fig. 4. IDA curves in terms of maximum interstory drift response. (a) $\delta^{(1)}_{max}$; (b) $\delta^{(2)}_{max}$; (c) $\delta^{(3)}_{max}$

6. Seismic fragility

The seismic fragility is defined as the probability P_f of exceeding limit states (LSs) in terms of increasing IM levels. The LS thresholds must be defined to construct the curves that represent the seismic fragility of the superstructure. In this study, 30 LS thresholds were defined for each EDP, ranging from $LS^{(i)}_{\delta_{max}} = 0.1\%$ to $LS^{(i)}_{\delta_{max}} = 1.5\%$. The probabilities of exceeding the defined LS thresholds at each IM level were computed by employing lognormal complementary cumulative distribution functions. The total probability theorem was used to consider the collapse and not-collapse simulations in the probabilistic assessment. In Fig. 5, the first inter-story fragility curves of the three considered isolation systems related to LS thresholds of 0.5%, 1%, and 1.5% are shown. The larger the value of the LS threshold, the lower fragility curves are obtained. In general, using LIR-DCFP bearings decreases the probabilities of exceeding different maximum inter-story drift thresholds. This decrement rises for larger values of the threshold. In Fig. 5, it is possible to note that using a larger DCFP bearing decreases the fragility, but this alternative is less efficient than using the novel frictional isolator.

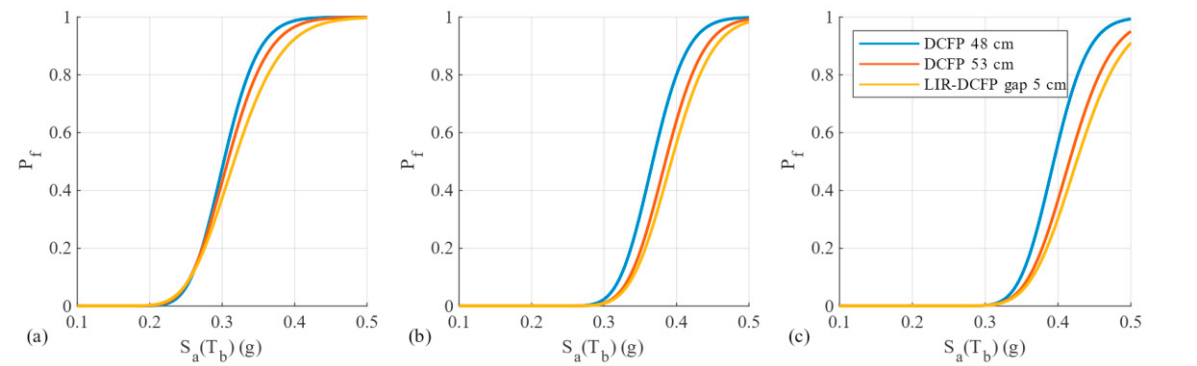

Fig. 5. Seismic fragility curves. (a) $\delta^{(1)}_{max}$; (b) $\delta^{(2)}_{max}$; (c) $\delta^{(3)}_{max}$

7. Seismic reliability

The annual rate of exceeding LS thresholds λ_{LS} can be determined through the convolution integral between the fragility curves ante the seismic hazard curve, as follow:

$$\lambda_{LS}(EDP > y) = \int_0^{\infty} P(EDP > y \mid S_a(T_b) = x)|\lambda(dS_a(T_b) > x)| \quad (2)$$

in which $P(EDP > y \mid S_a(T_b) = x)$ represents the calculated fragility curves, and $|\lambda(dS_a(T_b) > x)|$ represents the derivative of the hazard curve multiplied by an increment $dS_a(T_b)$. Using the annual rate of exceeding LS threshold λ_{LS} and a Poisson distribution, it is possible to determine the seismic reliability in the life-lime of the structure (i.e., 50 years):

$$P_f(50\ years) = 1 - exp\left(-\lambda_{LS} \cdot (50\ years)\right) \quad (3)$$

In Fig. 6, the reliability curves related to the superstructure in terms of maximum inter-story drift are plotted on a logarithmic scale for the three studied dynamic systems. The curves related to the isolation system formed by LIR-DCFP bearings tend to be below the curves related to base-isolated structures equipped with classic DCFP bearings, showing that using frictional isolators with high-friction interfaces decreases the probabilities of exceeding maximum inter-story drift LS thresholds. The lower probabilities of observing large values of maximum inter-story drift are expressed in better seismic performance. While reductions in the maximum first inter-story drift (critical story) up to 29% are achieved by replacing DCFP isolators with same-size LIR-DCFP bearings, reductions of only 20% are achieved by increasing the size of concave plates of DFCP devices.

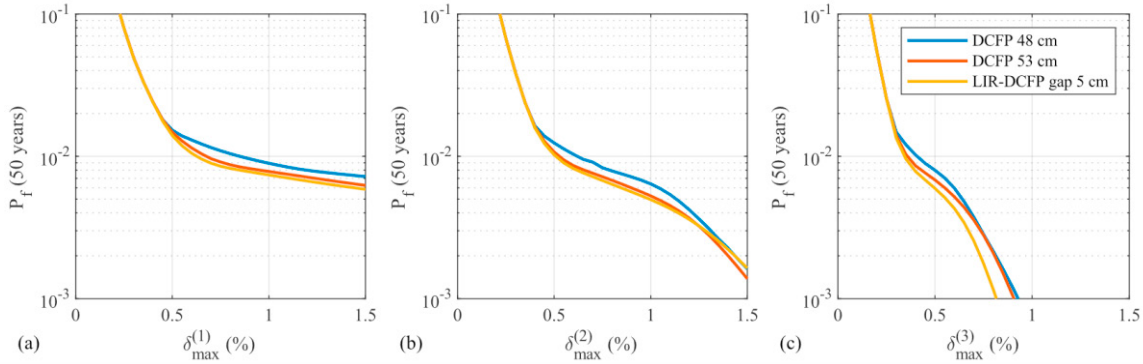

Fig. 6. Seismic reliability curves. (a) $\delta_{max}^{(1)}$; (b) $\delta_{max}^{(2)}$; (c) $\delta_{max}^{(3)}$

8. Conclusions

This article presents a reliability-based comparison of the seismic performance of an ordinary moment-resisting reinforced concrete frame equipped with different configurations of seismic isolators. Three isolations systems were considered, two formed by DCFP bearings (one with a larger lateral capacity). The third isolation system is composed of novel frictional isolators capable of resisting internal lateral impacts. The Lateral Impact Resilient Double Concave Friction Pendulum (LIR-DCFP) bearing has an improved inner slider with a high-friction interface. The impact between the inner slider and the restraining rims of the concave plates triggers the relative displacement along with the high-friction interface, limiting the maximum magnitude of the impact and dissipating an additional amount of energy. The mechanism exhibited by the improved inner slider has been suggested as an alternative to mitigate the adverse effects of internal impacts. One of these effects is a dramatic rise in the maximum inter-story drift response. This study aims to compare the reduction of this Engineering Demand Parameter when LIR-DCFP devises are used.

Completely nonlinear models were developed to analyze the dynamic behavior of the isolated building. While the superstructure was modeled considering geometric and material nonlinearities through the use of degrading beam-columns elements in state-space form, the isolation devices were implanted using an approach based on rigid body dynamics. This approach allows to effectively incorporate the lateral impact behavior of the bearings and

mechanisms of bearing failure. The dynamic response of the superstructure equipped with three configurations of isolation systems in terms of maximum inter-story drifts was statistically characterized by performing Incremental Dynamic Analyses (IDAs). With the data generated in the IDAs and defining limit state (LS) thresholds, fragility curves related to the maximum inter-story drift were constructed. Finally, through the convolution integral between the fragility curves and the hazard curve of a site in Riverside (California), reliability curves in a time frame of 50 years were derived. These reliability curves are a valuable tool for comparing the seismic performance of different isolation systems. Reductions up to 29% in the maximum first story drift (the critical story) are achieved by replacing classical Double Concave Friction Pendulum (DCFP) with same-size LIR-DCFP isolators. Reductions of only 19% are obtained by increasing the size of the concave plate of DCFP bearings. Hence, a high-friction interface as a mechanism to mitigate the adverse effects of internal lateral impacts is more effective than increasing the lateral capacity of classical frictional isolators.

Acknowledgements

This research has been funded by the National Agency for Research and Development (ANID) through the ANID-PCHA/Doctorado Nacional/2018-21180434 and the FONDECYT project Nº1201841, the authors are grateful for the support.

References

Auad, G., & Almazán, J. L., 2021. Lateral Impact Resilient double concave Friction Pendulum (LIR-DCFP) bearing: Formulation, parametric study of the slider and three-dimensional numerical example. Engineering Structures, 233, 111892.

Bao, Y., Becker, T. C., & Hamaguchi, H., 2017. Failure of double friction pendulum bearings under pulse-type motions. Earthquake Engineering & Structural Dynamics, 46(5), 715-732.

Bao, Y., & Becker, T. C., 2018. Effect of design methodology on collapse of friction pendulum isolated moment-resisting and concentrically braced frames. Journal of Structural Engineering, 144(11), 04018203.

Becker, T. C., Bao, Y., & Mahin, S. A., 2017. Extreme behavior in a triple friction pendulum isolated frame. Earthquake Engineering & Structural Dynamics, 46(15), 2683-2698.

Bao, Y., & Becker, T., 2019. Three-dimensional double friction pendulum bearing model including uplift and impact behavior: Formulation and numerical example. Engineering Structures, 199, 109579.

Constantinou, M., Mokha, A., & Reinhorn, A., 1990. Teflon bearings in base isolation II: Modeling. Journal of Structural Engineering, 116(2), 455-474.

Fenz, D. M., & Constantinou, M. C., 2006. Behaviour of the double concave friction pendulum bearing. Earthquake engineering & structural dynamics, 35(11), 1403-1424.

Fenz, D. M., & Constantinou, M. C., 2008. Spherical sliding isolation bearings with adaptive behavior: Experimental verification. Earthquake engineering & structural dynamics, 37(2), 185-205.

Hall, J. F., Heaton, T. H., Halling, M. W., & Wald, D. J., 1995. Near-source ground motion and its effects on flexible buildings. Earthquake spectra, 11(4), 569-605.

Mazza, F., & Vulcano, A., 2012. Effects of near-fault ground motions on the nonlinear dynamic response of base-isolated rc framed buildings. Earthquake Engineering & Structural Dynamics, 41(2), 211-232.

Mazza, F., 2018. Seismic demand of base-isolated irregular structures subjected to pulse-type earthquakes. Soil Dynamics and Earthquake Engineering, 108, 111-129.

Mokha, A., Constantinou, M., & Reinhorn, A., 1990. Teflon bearings in base isolation I: Testing. Journal of Structural Engineering, 116(2), 438-454.

Zayas, V. A., Low, S. S., & Mahin, S. A., 1990. A simple pendulum technique for achieving seismic isolation. Earthquake spectra, 6(2), 317-333.